Results in Physics 83 (2026) 108626

Contents lists available at ScienceDirect

Results in Physics

journal homepage: www.elsevier.com/locate/rinp

Symmetry-balanced electronic structure, optical anisotropy and lattice dynamics of equiatomic In–Ga–Se: A first-principles study

Z.A. Jahangirli [a,b], K.K. Azizova [a,c], T.K. Nurubeyli [a,d,e,*], U.I. Ashurova [f], N.V. Kerimli [g], G.N. Mammadova [h], S.S. Osmanova [i], N.V. Kazimova [j], L.V. Mammadov [k], T.O. Bayramova [b]

[a] Institute of Physics of the Ministry of Science and Education of Republic of Azerbaijan, H. Javid Avenue, 131, Baku AZ-1073, Azerbaijan
[b] Baku State University, Baku AZ1148, Azerbaijan
[c] Western Caspian University, Baku, Azerbaijan
[d] Azerbaijan State Oil and Industry University, Azadliq Avenue, 20, Baku AZ-1010, Azerbaijan
[e] Khazar University, Mahsati Str. 41, Baku, AZ 1096, Azerbaijan
[f] Mingachevir State University, Mingachevir, Azerbaijan
[g] Azerbaijan Medical University, Samad Vurgun st.167, Baku Az1022, Azerbaijan
[h] Nakhchivan State University, A. Aliyev 11, AZ7000 Nakhchivan city, Azerbaijan
[i] Azerbaijan Technical University, Baku AZ1143, Azerbaijan
[j] Azerbaijan University of Technology, Ganja, Azerbaijan
[k] Baku Engineering University, Baku, Azerbaijan

ARTICLE INFO

Keywords:
Equiatomic In–Ga–Se alloy
Layered chalcogenide semiconductors
Electronic structure
Optical anisotropy
Phonon dispersion
Raman spectroscopy
Density functional theory

ABSTRACT

Equiatomic cation ordering in layered III–VI chalcogenides provides a unique platform for disentangling the intrinsic coupling between electronic states, optical anisotropy, and lattice vibrations. In this work, $In_{0.5}Ga_{0.5}Se$ is employed as a symmetry-balanced reference system to clarify how equal In/Ga substitution modifies the microscopic origin of optical and vibrational responses in layered semiconductors.

First-principles calculations show that the equiatomic composition preserves a direct band gap of approximately 1.9 eV. The band-edge electronic structure is governed by hybridized Se p and In/Ga s states, which determine the symmetry-allowed optical transition channels and enhance the polarization-dependent dielectric response.

The calculated dielectric spectra reveal a pronounced contrast between in-plane and out-of-plane optical excitations. This anisotropy originates from symmetry-constrained interband transition channels and the preferential in-plane orientation of Se p orbitals, rather than from compositional asymmetry.

Phonon calculations combined with Raman spectroscopy further demonstrate that equiatomic cation balance leads to a characteristic redistribution of vibrational spectral weight, enabling reliable identification of Raman-active modes and their displacement patterns. The absence of imaginary phonon frequencies confirms the dynamical stability of the equiatomic lattice. The phonon-derived heat capacity follows Debye-like behavior at low temperatures and approaches the Dulong–Petit limit at elevated temperatures.

By isolating symmetry effects from compositional imbalance, the present results provide a physically transparent reference for understanding electronic–optical–phonon coupling in In–Ga–Se solid solutions and related layered chalcogenide semiconductors.

Introduction

Layered III–VI chalcogenide semiconductors constitute an important class of low-dimensional materials in which reduced dimensionality and anisotropic chemical bonding lead to strongly direction-dependent electronic, optical, and vibrational properties [1,2]. Owing to their layered crystal structures, these materials exhibit pronounced polarization sensitivity in optical excitation, large absorption coefficients in the visible range, and distinctive lattice dynamics governed by weak interlayer interactions. Such characteristics make layered chalcogenides

* Corresponding author at: Institute of Physics of the Ministry of Science and Education of Republic of Azerbaijan, H. Javid Avenue, 131, Baku AZ-1073, Azerbaijan.
E-mail address: t.nurubeyli@physics.science.az (T.K. Nurubeyli).

https://doi.org/10.1016/j.rinp.2026.108626
Received 6 January 2026; Received in revised form 20 February 2026; Accepted 8 March 2026
Available online 9 March 2026

particularly suitable for investigating fundamental coupling mechanisms between electronic states, optical response, and lattice vibrations in anisotropic solids.

Within this material family, the In–Ga–Se system is of special interest because substitution between indium and gallium offers a controllable route for modifying the electronic structure while preserving the underlying layered framework [3,4]. While the binary end members InSe and GaSe have been extensively studied, significantly less attention has been paid to compositions in which the cation sublattice is equally occupied. In particular, equiatomic $In_{0.5}Ga_{0.5}Se$ represents a symmetry-balanced configuration in which compositional disorder and crystallographic anisotropy coexist, providing a distinct physical environment compared to non-equiatomic solid solutions.

From a microscopic standpoint, equal In/Ga substitution influences the hybridization between chalcogen p states and cation s and p states near the band edges, thereby modifying optical transition probabilities and polarization-dependent dielectric response [5]. The layered crystal symmetry imposes strong selection rules on optical excitations and vibrational modes, resulting in a pronounced contrast between in-plane and out-of-plane responses. This contrast originates from the directional character of Se p orbitals and their preferential in-plane hybridization with In/Ga s states, which enhances in-plane optical transitions. In equiatomic compositions, these effects are governed primarily by symmetry constraints rather than compositional imbalance, offering an opportunity to isolate intrinsic anisotropy-related phenomena from concentration-driven effects.

First-principles approaches based on density functional theory (DFT) provide a robust framework for exploring these issues, allowing a unified and parameter-free description of electronic structure, optical spectra, and lattice dynamics [6,7]. Density-functional perturbation theory enables accurate calculation of phonon dispersions and vibrational symmetries, which can be directly compared with experimental Raman spectra. Such combined theoretical and experimental studies are essential for establishing reliable structure–property relationships in layered semiconductors and for validating microscopic interpretations of experimentally observed spectral features [6,8,9].

Despite these advances, comprehensive investigations that explicitly treat equiatomic In–Ga–Se compositions as symmetry-balanced reference systems remain scarce, particularly those combining detailed first-principles optical analysis with experimentally validated vibrational spectroscopy. Most existing works focus either on binary compounds or on non-equiatomic solid solutions, where compositional asymmetry often obscures intrinsic symmetry-driven effects. Consequently, the microscopic origin of optical anisotropy and its interplay with lattice dynamics in equiatomic $In_{0.5}Ga_{0.5}Se$ has not yet been systematically clarified.

In this work, we address this gap by performing a combined first-principles and experimental investigation of equiatomic $In_{0.5}Ga_{0.5}Se$. Using density functional theory together with density-functional perturbation theory and Raman spectroscopy, we analyze the electronic band structure, polarization-dependent optical response, and lattice dynamics of this material. By establishing $In_{0.5}Ga_{0.5}Se$ as a symmetry-balanced reference system within the In–Ga–Se family, the present study disentangles symmetry-controlled electronic–optical–phonon coupling from concentration-driven effects and provides a physically transparent framework applicable to related layered chalcogenide semiconductors.

Experimental and computational details

The electronic structure and optical properties of equiatomic $In_{0.5}Ga_{0.5}Se$ were calculated within the framework of density functional theory using the full-potential linearized augmented plane-wave (FP-LAPW) method, as implemented in the WIEN2k package [10]. The plane-wave cutoff was defined by RmtKmax = 7.0, while the partial-wave expansion inside the muffin-tin spheres included angular momentum components up to lmax = 10. Muffin-tin radii of 2.0 Bohr were adopted for In, Ga, and Se atoms. Core and valence states were separated by an energy threshold of − 6.0 Ry [11–13].

Brillouin-zone integrations were performed using the tetrahedron method [14] with a dense mesh of 2000 k-points in the irreducible Brillouin zone to ensure convergence of the charge density and total energy. Structural and electronic calculations were initially carried out using the generalized gradient approximation in the Perdew–Burke–Ernzerhof (PBE) form [15] for the exchange–correlation functional. To obtain a more reliable description of the band gap and optical transitions, the modified Becke–Johnson (mBJ) exchange potential was subsequently employed [16], which is known to provide improved band-gap estimates for semiconductors without introducing empirical parameters.

The equiatomic $In_{0.5}Ga_{0.5}Se$ composition was modeled using an ordered configuration in which In and Ga atoms occupy crystallographically distinct sites in a 1:1 ratio within the hexagonal lattice, preserving the overall symmetry of the parent structure.

The frequency-dependent dielectric function was calculated within the independent-particle approximation using momentum matrix elements between occupied and unoccupied electronic states. Intraband (Drude-like) contributions were not included, as the system is treated as a semiconductor without free carriers.

Lattice dynamical properties were investigated within density-functional perturbation theory (DFPT) using the plane-wave pseudopotential approach as implemented in the ABINIT code [17–19]. Norm-conserving Hartwigsen–Goedecker–Hutter pseudopotentials [20,21] were used in conjunction with the generalized gradient approximation for the exchange–correlation functional. The electronic wavefunctions were expanded in a plane-wave basis with an energy cutoff of 80 Ry, ensuring convergence of the total energy and phonon frequencies. Sampling of the Brillouin zone was performed using a Monkhorst–Pack k-point grid of 4 × 4 × 4 [22,23].

The equilibrium lattice parameters and internal atomic coordinates were obtained through full structural relaxation starting from the experimentally reported crystal structure. Geometry optimization was carried out by minimizing the Hellmann–Feynman forces using the Broyden–Fletcher–Goldfarb–Shanno (BFGS) algorithm until the residual forces on all atoms were reduced below 10^{-4} eV $Å^{-1}$. Prior to the final calculations, systematic convergence tests with respect to k-point sampling and plane-wave cutoff were performed to ensure an optimal balance between numerical accuracy and computational efficiency.

Experimental Raman measurements

Raman spectra of hexagonal $In_{0.5}Ga_{0.5}Se$ were recorded at room temperature using a confocal Raman microspectrometer (Nanofinder 30, Tokyo Instruments, Japan) in the backscattering geometry. A Nd:YAG laser operating at 532 nm was used as the excitation source. The laser power at the sample surface was limited to 1 mW to prevent local heating effects. The spectral resolution was better than 0.5 cm^{-1}. The scattered signal was detected using a thermoelectrically cooled charge-coupled device (CCD) operating at − 100 °C. All measurements were performed under unpolarized conditions.

Results and discussion

Electronic structure and optical properties

Local and semi-local exchange–correlation functionals are known to systematically underestimate the fundamental band gaps of semiconductors due to the absence of the derivative discontinuity in the exchange–correlation potential. To obtain a reliable description of the electronic structure relevant for optical excitations, the modified Becke–Johnson (mBJ) potential was therefore employed, which has been demonstrated to yield accurate band gaps for a wide range of

semiconducting materials.

The calculated electronic band structures of equiatomic $In_{0.5}Ga_{0.5}Se$ obtained within the GGA and mBJ frameworks are shown in Fig. 1. Both approaches consistently predict a direct band gap with the valence-band maximum and conduction-band minimum located at the Γ point, reflecting the symmetry of the layered crystal structure. The application of the mBJ potential leads to a substantial widening of the band gap, resulting in a value of approximately 1.9 eV, which is well suited for optical transitions in the visible range. The preservation of direct-gap character upon band-gap correction confirms that the essential features of the electronic dispersion are governed by crystal symmetry rather than by the choice of exchange–correlation functional.

The calculated direct band gap of ~ 1.9 eV is consistent with reported experimental trends for related In–Ga–Se solid solutions. Although the present study primarily focuses on first-principles optical predictions, future polarization-resolved optical measurements would provide further experimental validation of the predicted anisotropic dielectric response.

Insight into the microscopic origin of the electronic states is provided by the atom-projected density of states shown in Fig. 2. The upper valence band is dominated by Se 4p states strongly hybridized with In 5p and Ga 4p orbitals, indicating significant covalent character of the bonding within the layers. In contrast, the conduction-band minimum is primarily composed of In 5 s and Ga 4 s states with a smaller contribution from Se 4p orbitals. This p–s type band-edge configuration is characteristic of layered III–VI chalcogenides and plays a decisive role in determining the optical selection rules and transition strengths. Deep-lying states observed around − 14 eV originate mainly from Se 4 s orbitals and do not participate in low-energy optical excitations.

The polarization-dependent dielectric response further reflects the layered nature of $In_{0.5}Ga_{0.5}Se$. The real and imaginary parts of the dielectric function for in-plane (ε||) and out-of-plane (ε⊥) light polarization are presented in Fig. 3. The imaginary component of ε|| exhibits a pronounced maximum near 5.4 eV, accompanied by weaker features at higher energies, while the corresponding ε⊥ spectrum shows reduced intensity. These features arise from interband transitions between the Se p-dominated valence states and the In/Ga s-like conduction states, in agreement with the band-structure and PDOS analysis.

The pronounced optical anisotropy originates from the directional character of Se p orbitals and their preferential in-plane (p_x,p_y) hybridization with In/Ga s states within the basal plane. This stronger orbital overlap enhances the corresponding dipole transition matrix elements for in-plane polarization, leading to dominant ε|| contributions. In contrast, out-of-plane transitions involve weaker overlap of p_z orbitals, resulting in reduced ε⊥ intensity. Thus, the anisotropic dielectric response is a direct consequence of symmetry-constrained orbital orientation rather than compositional imbalance.

It should be emphasized that, due to the hexagonal crystal symmetry (C6v), the in-plane dielectric tensor components εxx and εyy are symmetry-equivalent. Therefore, no intrinsic anisotropy is expected within the basal plane itself. The observed optical anisotropy refers exclusively to the contrast between in-plane (ε||) and out-of-plane (ε⊥) polarization directions.

In Fig. 3 the real part of the dielectric function, Re(ε), exhibits zero-crossing points at high photon energies: Re(ε||) crosses zero at ≈5.5 eV and Re(ε⊥) at ≈6.8 eV. These zero crossings correspond to screened, plasma-like resonant conditions of the interband response, i.e., energies at which the collective interband polarization becomes sufficiently strong that the real part of the permittivity changes sign and the material response acquires a metal-like character. Because $In_{0.5}Ga_{0.5}Se$ is a semiconductor with negligible free-carrier density in our calculations, these features originate from strong interband transition contributions to the dielectric function rather than from free-carrier (Drude) plasmons. The Re(ε) = 0 condition therefore marks the energy region where longitudinal collective excitations may occur and where reflectivity is enhanced (Figs. 4-7).

The absorption coefficients coincide with the direct mBJ band gap of ≈1.9 eV: Im(ε) rises above the gap and the absorption coefficient reaches values of order 10^4–10^5 cm^{-1}, confirming strong allowed interband absorption. The refractive index near the band edge attains static values of approximately 3.8 for both polarizations, while Re(ε) remains positive throughout the visible region, indicating dielectric behavior. The observed polarization dependence of the absorption edge and related optical constants is attributed to symmetry-constrained transition matrix elements between Se-p dominated valence bands and In/Ga-s dominated conduction bands; this microscopic origin underlies the

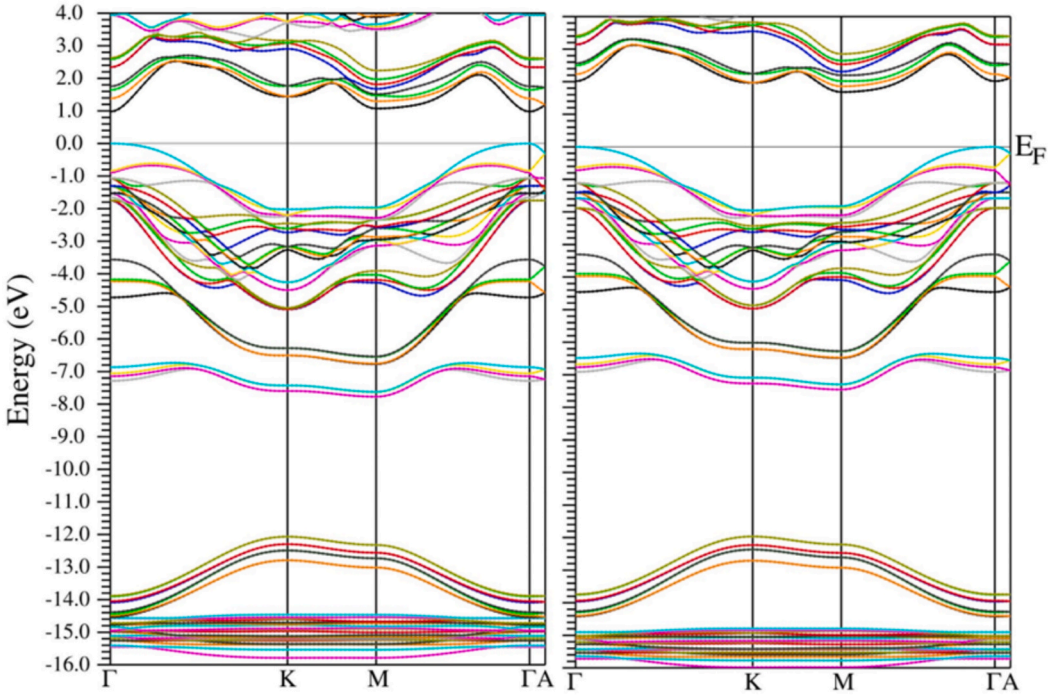

Fig. 1. Electronic band structures of equiatomic $In_{0.5}Ga_{0.5}Se$ calculated within (a) GGA and (b) GGA + mBJ approaches, showing a direct band gap at the Γ point.

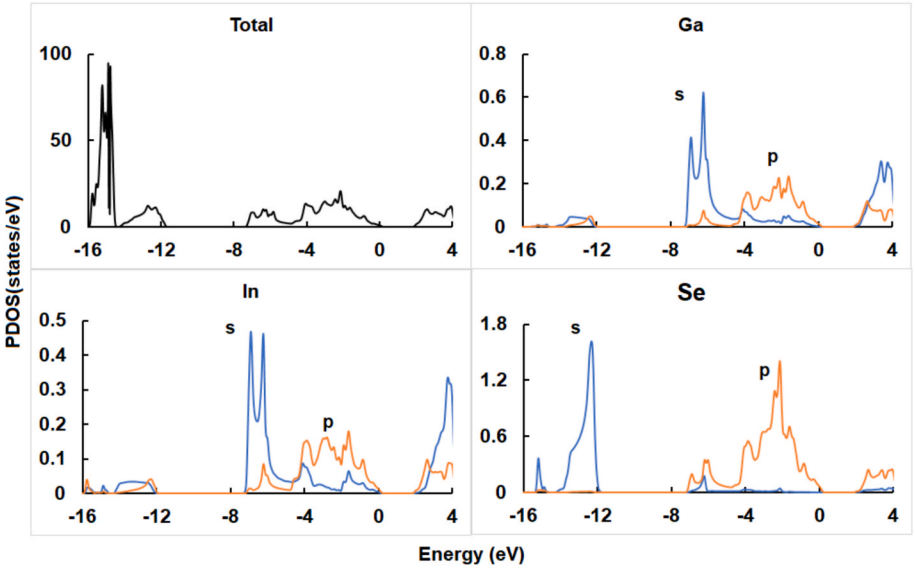

Fig. 2. Atom-resolved partial density of states of $In_{0.5}Ga_{0.5}Se$ calculated using the GGA + mBJ potential, highlighting the p–s hybridization at the band edges. The Fermi level is set to zero energy.

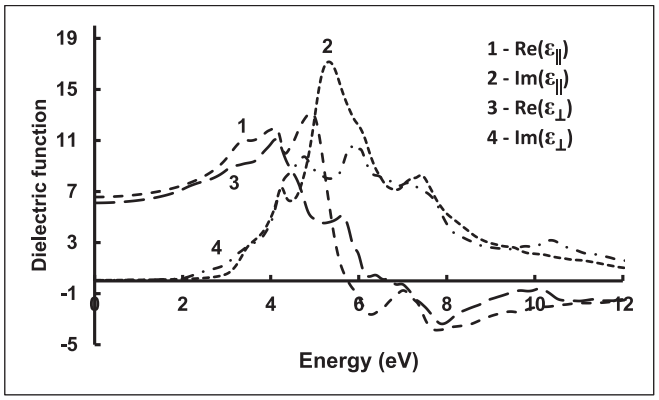

Fig. 3. Real and imaginary parts of the dielectric function of $In_{0.5}Ga_{0.5}Se$ for light polarized parallel (ε||) and perpendicular (ε⊥) to the crystallographic c-axis, illustrating pronounced optical anisotropy.

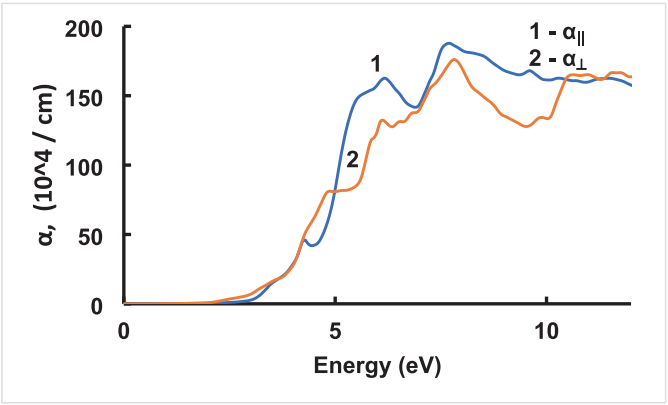

Fig. 5. Absorption coefficient spectra of $In_{0.5}Ga_{0.5}Se$ for different light polarizations, demonstrating strong direct interband absorption in the visible and ultraviolet regions.

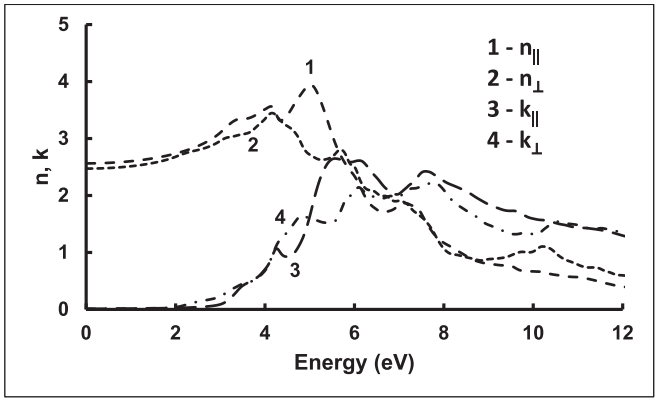

Fig. 4. Spectral dependence of the refractive index (n) and extinction coefficient (k) of $In_{0.5}Ga_{0.5}Se$ for in-plane (E ⊥ c) and out-of-plane (E || c) light polarizations.

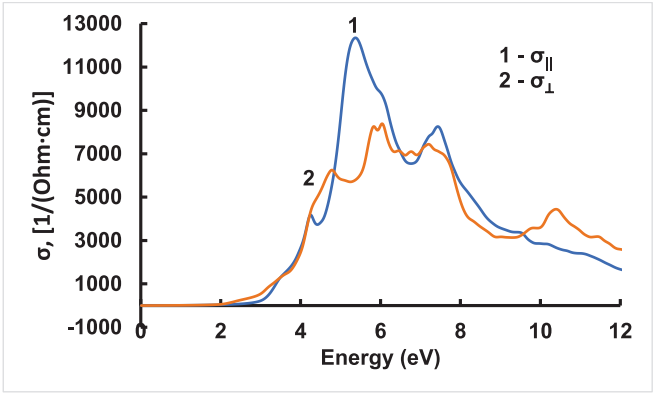

Fig. 6. Real part of the optical conductivity of $In_{0.5}Ga_{0.5}Se$ for in-plane and out-of-plane polarizations, revealing intense interband transition peaks in the 3.5–7 eV range.

pronounced anisotropy between ε|| and ε⊥ in the visible spectral window.

The calculated refractive index, extinction coefficient, absorption coefficient, optical conductivity, and reflectivity spectra are presented in

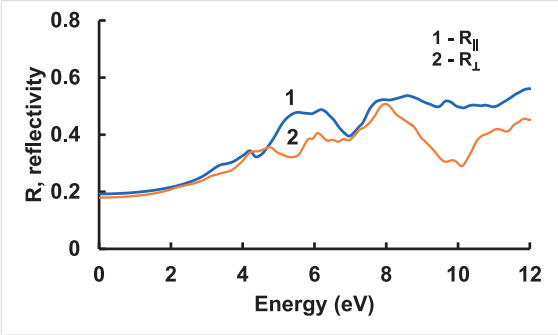

Fig. 7. Reflectivity spectra of $In_{0.5}Ga_{0.5}Se$ for light polarized parallel and perpendicular to the layers, showing enhanced reflectance in the ultraviolet region due to strong interband transitions.

Figs. 4–7. The refractive index reaches its maximum values in the near-ultraviolet region and decreases at higher photon energies, while the extinction coefficient remains negligible below the band edge and rises sharply once direct interband transitions become allowed. The static refractive indices for both polarizations are approximately 3.8, reflecting the relatively high polarizability of the layered structure.

A large absorption coefficient on the order of 10^4–10^5 cm^{-1} is observed in the energy range from 2 to 5 eV (Fig. 5), confirming that optical absorption is dominated by direct allowed transitions near the fundamental band gap. The real part of the optical conductivity (Fig. 6) exhibits pronounced peaks between approximately 3.5 and 7 eV, with the in-plane component carrying the dominant spectral weight. These conductivity maxima are directly correlated with the peaks in the imaginary part of the dielectric function and are responsible for the strong ultraviolet absorption and enhanced reflectivity in this energy region.

The reflectivity spectra (Fig. 7) display relatively low reflectance below the optical gap, followed by a monotonic increase toward the ultraviolet, reaching values of about 0.5–0.6 at energies corresponding to intense interband transitions. The polarization dependence of the reflectivity mirrors that of the dielectric and conductivity spectra, reinforcing the conclusion that optical anisotropy in $In_{0.5}Ga_{0.5}Se$ originates from the combined effects of layered crystal symmetry and band-edge orbital hybridization.

The present calculations correspond to the bulk hexagonal phase of $In_{0.5}Ga_{0.5}Se$. In reduced-dimensional systems (e.g., few-layer structures), quantum confinement effects may modify the magnitude of the band gap and the energy position of optical features. Nevertheless, the dominant in-plane orbital hybridization responsible for the anisotropic dielectric response is expected to remain qualitatively preserved due to the layered bonding topology.

Although direct optical absorption measurements were not performed in this work, previously reported optical studies on related In–Ga–Se compositions confirm direct band gap behavior in the 1.8–2.0 eV range [11]. Therefore, the present theoretical results are consistent with available experimental trends.

Lattice dynamics and Raman spectra

The lattice dynamical properties of equiatomic $In_{0.5}Ga_{0.5}Se$ were analyzed on the basis of crystal symmetry and first-principles phonon calculations. The compound crystallizes in the hexagonal structure with space group $P6_3mc$ (No. 186), corresponding to the C_{6v} (6 mm) point group. The primitive unit cell contains sixteen atoms, giving rise to forty-eight phonon modes at the Brillouin-zone center. Indium, gallium, and selenium atoms occupy the Wyckoff positions 2a and 2b, resulting in a rich spectrum of vibrational excitations governed by both in-plane and out-of-plane atomic motions.

Group-theoretical analysis yields the following decomposition of the Γ-point phonon modes:

$$\Gamma = 8A_1 + 8B_1 + 8E_2 + 8E_1$$

The acoustic contribution is given by $\Gamma\_acoustic = A_1 + E_1$, while the remaining modes constitute the optical spectrum:

$$\Gamma\_optic = 7A_1 + 8B_1 + 8E_2 + 7E_1$$

Among these, the A_1, E_1, and E_2 modes are Raman-active, whereas the polar A_1 and E_1 modes are additionally infrared-active. The A_1 modes are non-degenerate, while the E_1 and E_2 modes are doubly degenerate, reflecting the underlying hexagonal symmetry.

The character of the vibrational modes is closely related to the layered crystal structure. The atomic displacements associated with the E_1 and E_2 modes are confined predominantly within the basal plane, whereas the A_1 and B_1 modes involve atomic motions along the crystallographic c-axis. Furthermore, the A_1 and E_1 modes correspond to in-phase oscillations of atoms within the basis, while the B_1 and E_2 modes are characterized by antiparallel displacements, leading to distinct Raman selection rules and spectral signatures.

Representative atomic displacement patterns for selected A_1, E_1, and E_2 modes are illustrated schematically in Fig. 8, highlighting the symmetry-dependent in-plane and out-of-plane vibrational character. These displacement patterns provide direct microscopic insight into the polarization dependence of Raman activity.

The calculated phonon dispersion relations and atom-projected phonon density of states are shown in Figs. 9 and 10, respectively. The phonon spectrum exhibits clear separation into frequency regions associated with different atomic contributions. The low-frequency region below approximately 150 cm^{-1} contains the acoustic branches and low-lying optical modes and is dominated by vibrations of the heavier In and Se atoms, with pronounced features near 60, 72, and 114 cm^{-1}. In the intermediate frequency range, Se vibrations remain predominant, while the highest-frequency optical modes around 259 cm^{-1} originate mainly from Ga atomic motion, reflecting the lower atomic mass of gallium. This separation of vibrational contributions provides a transparent microscopic interpretation of the phonon spectrum.

Importantly, the phonon dispersion curves do not exhibit imaginary frequencies at the Γ point or along high-symmetry directions, confirming the dynamical stability of the equiatomic lattice.

Experimental Raman spectra of hexagonal $In_{0.5}Ga_{0.5}Se$ are presented in Fig. 11 and compared with the calculated phonon frequencies summarized in Table 1. Only the most intense modes were observed experimentally.

The remaining theoretically predicted Raman-active modes, particularly several E_2 modes, were not clearly resolved in the experimental spectrum. This may be attributed to their relatively low Raman scattering cross-section, partial spectral overlap with neighboring peaks, and the use of an unpolarized measurement geometry. Additionally, weak modes located close in frequency may fall below the detection limit of the experimental configuration.

The close agreement between the experimentally observed A_1 (34, 109, 210, and 245 cm^{-1}) and E_1 (166 cm^{-1}) modes and their calculated counterparts confirms the reliability of the phonon calculations and allows unambiguous assignment of the observed Raman-active modes to specific vibrational symmetries and displacement patterns.

The average deviation between the calculated and experimentally observed frequencies for these modes is below 5%, indicating good quantitative agreement within the accuracy expected for density functional calculations.

Elastic properties were further evaluated to assess the mechanical stability of equiatomic $In_{0.5}Ga_{0.5}Se$. For hexagonal crystals, the elastic response is fully described by five independent elastic constants: C_{11}, C_{12}, C_{13}, C_{33}, and C_{44}. The mechanical stability of the structure was examined using the Born stability criteria for hexagonal systems [23–25]:

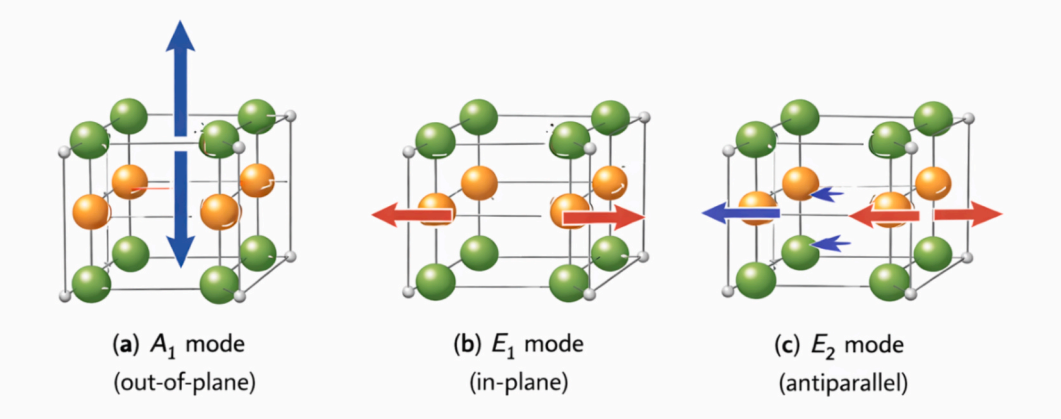

Fig. 8. Representative atomic displacement patterns of selected Raman-active phonon modes in equiatomic $In_{0.5}Ga_{0.5}Se$: (a) A_1 mode showing out-of-plane vibrations along the c-axis; (b) E_1 mode with in-plane atomic displacements; (c) E_2 mode characterized by in-plane antiparallel vibrations. Arrows indicate the direction of atomic motion.

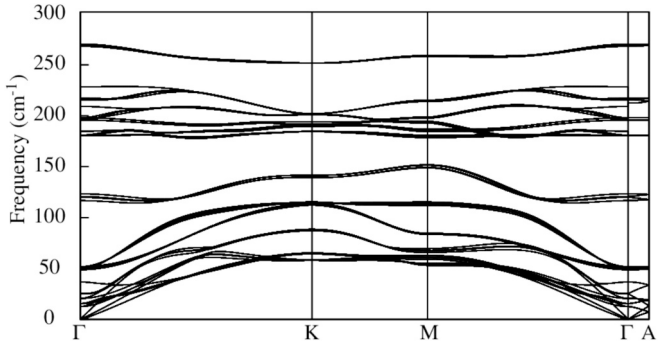

Fig. 9. Phonon dispersion relations of equiatomic $In_{0.5}Ga_{0.5}Se$ along high-symmetry directions of the Brillouin zone, confirming the absence of imaginary frequencies and dynamical stability of the lattice.

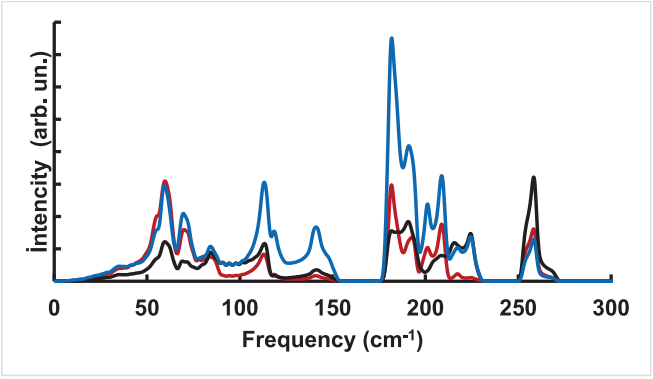

Fig. 10. Atom-projected phonon density of states of equiatomic $In_{0.5}Ga_{0.5}Se$, illustrating the contribution of In, Ga, and Se atoms to different vibrational frequency regions.

$C_{11} > |C_{12}|$, $C_{44} > 0$, $(C_{11} + C_{12})C_{33} > 2C_{13}^2$

The calculated elastic constants listed in Table 2 satisfy all stability conditions, demonstrating that equiatomic $In_{0.5}Ga_{0.5}Se$ is mechanically stable. The obtained values indicate moderate elastic anisotropy, consistent with the layered bonding topology and weak interlayer interactions.

The constant-volume heat capacity C_V was derived from the phonon density of states and is shown in Fig. 12. At low temperatures, C_V follows the Debye T^3 law, characteristic of acoustic phonon contributions. With increasing temperature, the heat capacity rises steadily and approaches the classical Dulong–Petit limit at high temperatures, reaching approximately 390 J mol^{-1} K^{-1} near 400 K. This behavior further confirms the dynamical stability of the lattice and the absence of low-energy soft modes.

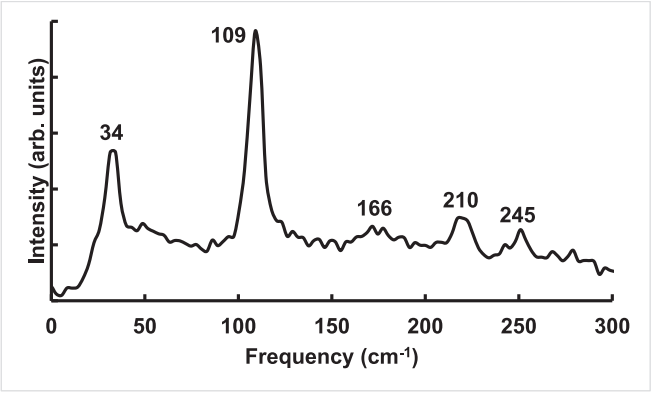

Fig. 11. Experimental Raman spectrum of hexagonal equiatomic $In_{0.5}Ga_{0.5}Se$ measured at room temperature, with assigned Raman-active vibrational modes.

Conclusion

A comprehensive first-principles and experimental investigation of equiatomic $In_{0.5}Ga_{0.5}Se$ has been carried out in order to clarify the relationship between electronic structure, optical anisotropy, and lattice dynamics in layered III–VI chalcogenide semiconductors. The calculations reveal that the equiatomic composition preserves a direct electronic band gap in the visible range, while exhibiting pronounced polarization-dependent optical response governed by the layered crystal symmetry.

Analysis of the electronic states demonstrates that the optical transitions near the band edges originate from hybridized cation–chalcogen states, providing a microscopic explanation for the strong in-plane optical absorption and anisotropic dielectric behavior. In particular, the dominant in-plane optical response arises from enhanced hybridization between Se p_x,p_y orbitals and cation s states, which increases the corresponding dipole transition matrix elements within the basal plane. The lattice dynamical properties, examined through density-functional perturbation theory and validated by Raman spectroscopy, confirm

Table 1
Calculated and experimentally observed Γ-point optical phonon frequencies of equiatomic $In_{0.5}Ga_{0.5}Se$, including mode symmetry and spectroscopic activity.

Mode symmetry	ωtheo (cm^{-1})	ωexp (cm^{-1})	Spectroscopic activity
A_1	36.8	34	Raman, IR
A_1	114.1	109	Raman, IR
A_1	123.3	—	Raman, IR
A_1	209.3	210	Raman, IR
A_1	217.4	—	Raman, IR
A_1	258.3	245	Raman, IR
A_1	270.3	—	Raman, IR
B_1	25.1	—	Silent
B_1	25.3	—	Silent
B_1	120.0	—	Silent
B_1	120.8	—	Silent
B_1	215.9	—	Silent
B_1	216.7	—	Silent
B_1	269.4	—	Silent
B_1	270.4	—	Silent
E_1	20.6	—	Raman, IR
E_1	48.8	—	Raman, IR
E_1	51.8	—	Raman, IR
E_1	174.5	166	Raman, IR
E_1	181.0	—	Raman, IR
E_1	196.0	—	Raman, IR
E_1	198.1	—	Raman, IR
E_2	12.6	—	Raman
E_2	15.5	—	Raman
E_2	50.2	—	Raman
E_2	50.8	—	Raman
E_2	180.6	—	Raman
E_2	180.9	—	Raman
E_2	195.9	—	Raman
E_2	198.1	—	Raman

Note: Raman-active modes are classified according to the irreducible representations of the C_{6v} point group. Experimental frequencies correspond to room-temperature Raman measurements.

Table 2
Independent elastic constants (in GPa) of equiatomic $In_{0.5}Ga_{0.5}Se$, demonstrating mechanical stability of the hexagonal lattice.

Compound	C_{11}	C_{12}	C_{13}	C_{33}	C_{44}
$In_{0.5}Ga_{0.5}Se$	86.5	25.2	15.3	37.5	11.5

Note: All elastic constants satisfy the Born stability criteria for hexagonal crystal systems, confirming mechanical stability of the equiatomic $In_{0.5}Ga_{0.5}Se$ phase.

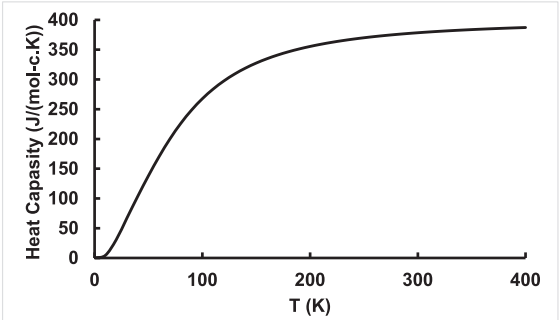

Fig. 12. Temperature dependence of the constant-volume heat capacity C_V of equiatomic $In_{0.5}Ga_{0.5}Se$ derived from phonon calculations, showing Debye-like behavior at low temperatures and saturation toward the Dulong–Petit limit at high temperatures.

the dynamical stability of the equiatomic lattice and allow reliable assignment of Raman-active vibrational modes based on symmetry and atomic displacement patterns.

The phonon spectrum exhibits a clear separation of vibrational contributions associated with different atomic species, reflecting the mass contrast between indium, gallium, and selenium atoms. In addition, the calculated elastic constants satisfy the Born stability criteria for hexagonal systems, indicating mechanical stability consistent with the absence of soft phonon modes. The temperature dependence of the heat capacity follows conventional Debye-like behavior at low temperatures and approaches the classical Dulong–Petit limit at elevated temperatures, further supporting the robustness of the lattice dynamics.

By isolating symmetry-driven effects from compositional imbalance, the present work establishes equiatomic $In_{0.5}Ga_{0.5}Se$ as a physically transparent reference system within the In–Ga–Se family. This approach enables a clearer understanding of how orbital orientation, crystal symmetry, and mass contrast collectively govern coupled electronic–optical–phonon phenomena in layered semiconductors. The results provide a reliable baseline for comparative investigations of compositional effects in the In–Ga–Se solid-solution family and related anisotropic semiconductor systems.

CRediT authorship contribution statement

Z.A. Jahangirli: Project administration, Formal analysis, Conceptualization. **K.K. Azizova:** Writing – review & editing, Methodology, Funding acquisition. **T.K. Nurubeyli:** Writing – original draft, Investigation, Conceptualization. **U.I. Ashurova:** Validation, Funding acquisition. **N.V. Kerimli:** Resources, Data curation. **G.N. Mammadova:** Supervision, Methodology. **S.S. Osmanova:** Visualization, Funding acquisition. **N.V. Kazimova:** Writing – review & editing, Software. **L.V. Mammadov:** Software, Resources. **T.O. Bayramova:** Writing – review & editing, Visualization.

Declaration of competing interest

The authors declare that they have no known competing financial interests or personal relationships that could have appeared to influence the work reported in this paper.

Data availability

The authors do not have permission to share data.

References

[1] Giri A, Park G, Jeong U. Layer-structured anisotropic metal chalcogenides: recent advances in synthesis, modulation, and applications. Chem Rev 2023;123(7): 3329–442. https://doi.org/10.1021/acs.chemrev.2c00455.
[2] Huang W, Gan L, Li H, Ma Y, Zhai T. Two-dimensional layered group IIIA metal chalcogenides: synthesis, properties and applications in electronics and optoelectronics. CrstEngComm 2016;18:3968–84. https://doi.org/10.1039/C5CE01986A.
[3] Ning CZ, Dou L, Yang P. Bandgap engineering in semiconductor alloy nanomaterials with widely tunable compositions. Nat Rev Mater 2017;2:17070. https://doi.org/10.1038/natrevmats.2017.70.
[4] Sato Y, Tang C, Watanabe K. Optical and electrical properties of $In_xGa_{1-x}Se$ mixed crystals grown from indium flux by the traveling heater method. J Electron Mater 2021;50:2649–55. https://doi.org/10.1007/s11664-020-08689-4.
[5] Liang WY. Optical anisotropy in layered compounds. J Phys C Solid State Phys 1973;6:551–9. https://doi.org/10.1088/0022-3719/6/3/018.
[6] Molina-Sánchez A, Wirtz L. Phonons in single-layer and few-layer MoS_2 and WS_2. Phys Rev B 2011;84:155413. https://doi.org/10.1103/PhysRevB.84.155413.
[7] Baroni S, de Gironcoli S, Dal Corso A, Giannozzi P. Phonons and related crystal properties from density-functional perturbation theory. Rev Mod Phys 2001;73: 515–62. https://doi.org/10.1103/RevModPhys.73.515.
[8] Yi J-X, et al. First-principles study of electronic structure and optical response in layered chalcogenide semiconductors. J Phys Condens Matter 2024;36:055501. https://doi.org/10.1088/1361-648X/ad05fc.
[9] Hasan M, Hossain AKMA, et al. First-principles investigation of electronic, optical and vibrational properties of layered materials. Results Phys 2022;42:106004. https://doi.org/10.1016/j.rinp.2022.106004.
[10] Blaha P, Schwarz K, Madsen GKH, Kvasnicka D, Luitz J. *WIEN2k: An augmented plane wave + local orbitals program for calculating crystal properties*. Vienna: Vienna University of Technology; 2008.
[11] Jahangirli ZA, Asadullayeva SG, Amiraslanov IR, et al. Ab initio and experimental investigations of the electronic and optical properties of pure and p-aminopyridine-

intercalated $In_{1.2}Ga_{0.8}S_3$. Indian J Phys 2025;99:2087–92. https://doi.org/10.1007/s12648-024-03452-5.
[12] Azizova KK, Jahangirli ZA, Ragimov SS, Nurubeyli TK, Suleymanova LC, Kerimli N, et al. Ab initio calculations of the electronic structure and optical properties of Cu_4SeTe crystals. Ukrainian Journal of Physical Optics 2025;26(4):4049–57. https://doi.org/10.3116/16091833/Ukr. J. Phys. Opt. 2025.04049.
[13] Cahangirli Z, Rahimli A, Mehdiyev B, et al. Electronic structure and optical properties of layered chalcogenides. Phys Solid State 2025;67(5):373–7. https://doi.org/10.1134/S1063783425600980.
[14] Blöchl PE, Jepsen O, Andersen OK. Improved tetrahedron method for Brillouin-zone integrations. Phys Rev B 1994;49:16223–33. https://doi.org/10.1103/PhysRevB.49.16223.
[15] Perdew JP, Burke K, Ernzerhof M. Generalized gradient approximation made simple. Phys Rev Lett 1996;77:3865–8. https://doi.org/10.1103/PhysRevLett.77.3865.
[16] Tran F, Blaha P. Accurate band gaps of semiconductors within a semilocal exchange–correlation potential. Phys Rev Lett 2009;102:226401. https://doi.org/10.1103/PhysRevLett.102.226401.
[17] Giannozzi P, de Gironcoli S, Pavone P, Baroni S. Ab initio calculation of phonon dispersions in semiconductors. Phys Rev B 1991;43:7231–42. https://doi.org/10.1103/PhysRevB.43.7231.
[18] Gonze X. Perturbation expansion of variational principles at arbitrary order. Phys Rev B 1997;55:10337–54. https://doi.org/10.1103/PhysRevB.55.10337.
[19] Gonze X, Lee C. Dynamical matrices, born effective charges, dielectric permittivity tensors, and interatomic force constants from density-functional perturbation theory. Phys Rev B 1997;55:10355–68. https://doi.org/10.1103/PhysRevB.55.10355.
[20] Gonze X, Beuken J-M, Caracas R, et al. First-principles computation of material properties: the ABINIT software project. Comput Mater Sci 2002;25:478–92. https://doi.org/10.1016/S0927-0256(02)00325-7.
[21] Hartwigsen C, Goedecker S, Hutter J. Relativistic separable dual-space Gaussian pseudopotentials. Phys Rev B 1998;58:3641–62. https://doi.org/10.1103/PhysRevB.58.3641.
[22] Monkhorst HJ, Pack JD. Special points for Brillouin-zone integrations. Phys Rev B 1976;13:5188–92. https://doi.org/10.1103/PhysRevB.13.5188.
[23] Mouhat F, Coudert F-X. Necessary and sufficient elastic stability conditions in various crystal systems. Phys Rev B 2014;90:224104. https://doi.org/10.1103/PhysRevB.90.224104.
[24] G.N. Mammadova, T.K. Nurubeyli, S.O. Gulieva, K.K. Azizova, S.J. Zeynalova "Dielectric and optical properties of Au-doped TlInSe2 for advanced optoelectronic devices" Physica B Condensed Matter, vol. 718, 417900, 2025 https://doi.org/10.1016/j.physb.2025.417900.
[25] Azizova KK, Jahangirli ZA, Nurubeyli TK, Suleymanova LC, Sultanova AH, Kerimli NV, et al. Electronıc, optıcal, and vıbratıonal properties ofLayered ın 0.3GA0.7SE: a dft and raman study. Ukrainian Journal of Physical Optics 2026;27(2):2043–57. https://doi.org/10.3116/16091833/Ukr.J.Phys.Opt.2026.02043.